Journal of ELECTRICAL ENGINEERING, VOL 59. NO 7/s, 2008, 37-40

MAGNETIC CHARACTERIZATION USING MINOR LOOP SCALING RULES

Satoru Kobayashi* − Seiki Takahashi*− Atsushi Saito*− Nobuhiro Kikuchi*− Hiroaki Kikuchi* − Yasuhiro Kamada* − Toetsu Shishido**

An universal scaling power-law rule of magnetic minor hysteresis loops, which is valid in all investigated materials, i.e. a relation between W_F* and M_R* is introduced. The relation gives an universal exponent of 1.4 and an obtained coefficient shows a similar behavior to the structure sensitive magnetic property, coercive force. Results for pure cobalt as well as strain-induced α'-martensites in 304-type stainless steels will be given as examples. This new scaling rule offers an opportunity for evaluating magnetic quality of materials, to which the existing scaling rules cannot be applied.

Keywords: magnetic minor hysteresis loops, nondestructive testing, scaling analysis, Cobalt, stainless steel

1 INTRODUCTION

Studies on scaling rules in magnetic hysteresis loops started about one century ago, because of increasing demand for electrical steels where accurate knowledge of power losses at high flux densities is particularly important. It is known that minor-loop hysteresis loss W_F^* is related to minor-loop magnetization, M_a^* at the medium range of M_a^*; $W_F^* \propto (M_a^*)^{1.6}$ [1]. This relation known as the Steinmetz law has been confirmed in various kinds of materials including iron, Permalloy, steels, ceramics, nanocrystalline alloy *etc*.

Recent our studies on single crystals of pure Fe and Ni showed that besides the Steinmetz law there exist another universal scaling relations between parameters of minor loops [2,3,4];

$$W_F{}^* = W_F{}^o \left(\frac{M_a{}^*}{M_S}\right)^{n_F}, \quad W_R{}^* = W_R{}^o \left(\frac{M_R{}^*}{M_R}\right)^{n_R},$$
$$H_c{}^* = H_c^o \left(\frac{M_R{}^*}{M_R}\right)^{n_C} \qquad (1)$$

Here, the first equation corresponds to the Steinmetz law and W_R^*, M_R^*, and H_c^* are remanence work, remanence, and coercive force of a minor loop, respectively. M_s and M_R are saturation magnetization and remanence of the major loop, respectively. W_F^0, W_R^0, and H_c^0 are minor-loop coefficients sensitive to internal stress due to lattice defects. Exponents n_F, n_R, and n_C are about 1.5, 1.5, and 0.45, respectively, being independent of temperature, stress, and kinds of lattice defects. This analysis method using scaling rules is advantageous for magnetic non-destructive testing because of its sensitivity to lattice defects and low measurements field.

Although the scaling rules hold true for almost ferromagnetic materials, it is known that there exist exceptional cases [5,6]. For instance, for polycrystals with strong magnetic anisotropy, a large deviation in the exponents was observed; n_F = 1.9 for pure Co [5]. This is attributed to the fact that magnetic response under a given external field is largely different from grain to grain and observed hysteresis loops are a mixture of hysteresis loops with various shape. On the other hand, the scaling rules do not hold true if there exists a large paramagnetic contribution as in the case of ferromagnetic α'-martensites formed in paramagnetic austenitic matrix.

In this paper, we propose a new universal scaling rule which is valid in all investigated materials, i.e. a relation between W_F^* and M_R^*. The relation gives an universal power-law exponent of 1.4 and an obtained coefficient shows a similar behaviour to other coefficients. Results for pure Co as well as strain-induced α'-martensites in 304-type stainless steels will be given as examples. This new scaling rule offers an opportunity for evaluating magnetic quality of materials, to which the existing scaling rules cannot be applied.

2 EXPERIMENTAL PROCEDURE

Toroidal samples of Co polycrystal with a purity of 99.9% and the single crystal grown from electron-beam FZ melting were prepared. A 80-turn exciting coil and a 80-turn pickup coil were wound around the samples with external and internal diameters of 9 mm and 7 mm, respectively, and thickness of 5 mm. The samples were placed in a He-gas closed-cycle refrigerator with a high-temperature stage, by which the temperature was varied from 10 to 700 K.

Slabs of 304 stainless steels with a thickness of 5 mm were austenitized at 1050 °C for 1 h, followed by the water quench. The slabs were then plastically deformed in tension at room temperature, with various levels of tensile stress up to 535 MPa. We prepared two types of samples for each stress; toroidal samples wound with 220-turn exciting and 120-turn pickup coils and small plates with the long axis parallel to the stress direction.

The plates were used to determine the volume fraction of α'-martensites by saturation magnetization

* NDE&Science Research Center, Faculty of Engineering, Iwate University, Morioka 020-8551, Japan; koba@iwate-u.ac.jp ** Institute for Materials Research, Tohoku University, Sendai 980-8577, Japan

ISSN 1335-3632

measurements using a superconducting quantum interference device (SQUID) magnetometer (Quantum Design MPMS-XL). A saturation magnetization of 154 emu/g was assumed for a volume fraction of 100%. The volume fraction of α'-martensites increases with stress and reaches 19.5% after plastic deformation by the maximum stress of 535 MPa (the inset in Fig. 5).

A set of magnetic minor hysteresis loops with various field amplitudes H_a up to ~ 20 kA/m was measured using a fluxmeter, for the toroidal samples. A cyclic magnetic field with H_a and a frequency of 0.2 Hz was applied in a demagnetized state and a minor loop, which is symmetric about the origin, was measured. By increasing H_a step-by-step, a set of minor loops was obtained. These minor loops are different from the major loop obtained with H_a that is sufficiently large for saturation.

3 EXPERIMENTAL RESULTS

3.1 Co polycrystal and single crystal

From a set of symmetrical minor loops with various H_a, the parameters such as W_F^* and M_a^* were obtained for each minor loop and scaling relations between the parameters were examined. Figures 1(a) and 1(b) show the double logarithmic plots of the relation between W_F^* and M_a^* for Co poly- and single crystals, respectively, taken at various temperatures. W_F^*-M_a^* curves show a straight line in a limited range of M_a^* and the slope is weakly temperature dependent for both materials, indicating the presence of a power-law rule between these parameters. Least-squares fits to (1) yielded a much higher value of $n_F = 2.1 \pm 0.1$ for Co polycrystal, whereas that for Co single crystal was 1.51 ± 0.03, being consistent with the value for Fe and Ni [2,3,4]. The large deviation of n_F from 1.6 for the Co polycrystal is possibly due to strong uniaxial anisotropy which results in a largely different microscopic hysteresis loops for each grain during a field cycle with H_a.

To explain these observations, we now consider the Rayleigh law [7]. At low fields, the magnetization process is determined by the displacements of domain walls and is well described by the Rayleigh law

$$M = \chi_a H + \frac{b}{2} H^2 \tag{2}$$

Here, χ_a is the initial susceptibility and describes the reversible part of magnetization, whereas the Rayleigh constant b, which is the structure-sensitive property, is related to the irreversible movement of domain walls. When a cyclic field with a small amplitude H_a is applied and the variation of the magnetization M with the field H follows (2), M_a^* and W_F^* are given, using H_a, by

$$M_a^* = \chi_a H_a + b H_a^2 , \quad W_F^* = \frac{4}{3}\mu_0 b H_a^3 \tag{3}$$

respectively. In soft ferromagnets, (3) always holds true, while for ferromagnets with large anisotropy, parameters of the Rayleigh law will be given by the summation of those due to each grain; $\chi_a = \Sigma\chi_{a,i}$, $b = \Sigma b_i$ where $\chi_{a,i}$ and

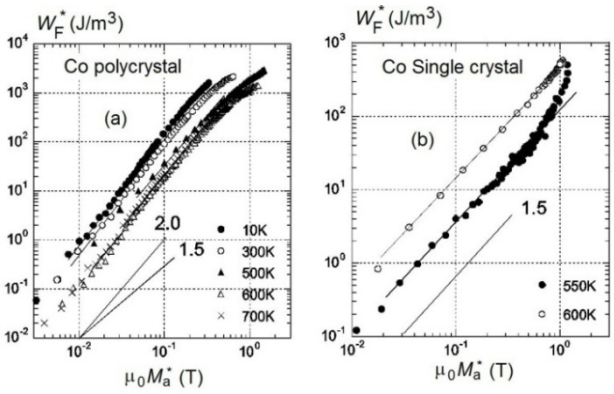

Fig. 1. The relation between W_F^* and M_a^* for (a) Co polycrystal and (b) its single crystal, taken for various temperatures. The solid lines through the data show the least-squares fit. Note that reliable data for Co single crystal were obtained only around 600 K where the irreversible movement of domain walls becomes dominant as compared to domain rotation owing to the strongly temperature dependent anisotropy.

b_i are the parameters for i-th grain. These equations give the relation between M_a^* and W_F^* as

$$W_F^* = \frac{\mu_0}{6\left(\sum b_i\right)^2}\left(-\sum \chi_{a,i} + \sqrt{\left(\sum \chi_{a,i}\right)^2 - 4M_a^* \sum b_i}\right)^3 \tag{4}$$

If domain wall movement is completely reversible for each grain, (4) yields $W_F^* \propto (M_a^*)^3$, while $W_F^* \propto (M_a^*)^{3/2}$ and the Steinmetz law holds true in the case of the irreversible movement. However, for Co polycrystals, magnetic response against applied fields varies from grain to grain owing to large magnetocrystalline anisotropy and the power-law exponent is always the intermediate value between 3/2 and 3 as was observed experimentally. The exponent depends on the strength of magnetocrystalline anisotropy and the Steinmetz law no longer holds true. This is unfavorable for accurate characterization of magnetic quality in ferromagnetic materials.

On the other hand, the remanence of minor loops, M_R^*, obtained from the Rayleigh law is given by

$$M_R^* = \frac{1}{2} b H_a^2 \tag{5}$$

and does not include χ_a explicitly. Using (3) and (5), the relation between W_F^* and M_R^* is expressed as

$$W_F^* = \frac{4}{3}\mu_0 \frac{\left(2M_R^*\right)^{3/2}}{\left(\sum b_i\right)^{1/2}} \tag{6}$$

This scaling rule only includes the information on b_i and therefore will hold true, irrespective of a microscopic magnetic state for each grain, namely, whether the domain wall movement for each grain is in the reversible or irreversible region.

Figures 2(a) and 2(b) show the double logarithmic plots of the relation between W_F^* and M_R^* for Co poly- and single crystals, respectively. The W_F^*-M_R^* curves exhibit a straight line in a limited range of M_R^*, but in this case the linearity persists even for minor loops with

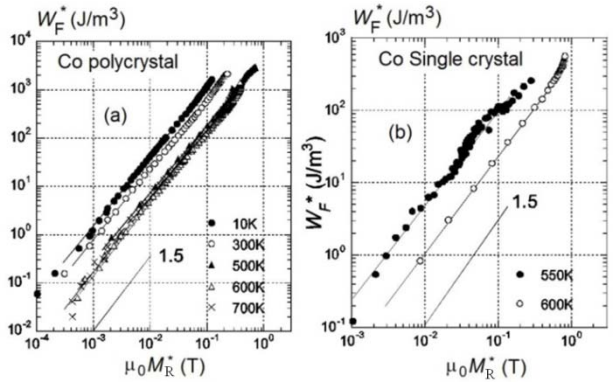

Fig. 2. The relation between W_F^* and M_R^* for (a) Co polycrystal and (b) its single crystal, taken for various temperatures. The solid lines through the data show the least-squares fits.

very low value of H_a. This linearity indicates the presence of a power-law rule between W_F^* and M_R^*. In order to extract the intrinsic magnetic properties of the relation, we assume an equation given as

$$W_F^* = W_m^0 \cdot \left(\frac{M_R^*}{M_R} \right)^{n_m}, \qquad (7)$$

where W_m^0 and n_m are a coefficient and power-law exponent, respectively. Least-squares fits to (7) gave an almost constant value of n_m = 1.41 ± 0.03 and 1.43 ± 0.01 for Co poly- and single crystals, respectively. Reanalysis of previous data for Ni polycrystals [4] using (7) also yielded a similar value of n_m = 1.34 ± 0.06. These results strongly indicate that the value of n_m is about 1.4 and universal, being independent of types of ferromagnets and temperature.

3.2 304-type stainless steel

Unlike ferromagnetic materials, 304 stainless steel includes a paramagnetic phase due to the austenitic matrix. In addition, strain-induced α'-martensites are magnetically hard as compared to ferromagnetic materials such as Fe and Ni. Therefore, the observed hysteresis loops are affected by the paramagnetic austenitic matrix and applied fields in addition to the ferromagnetic α'-martensites. The magnetic flux density B_{obs} observed by measurements is no longer approximated by $\mu_0 M$ due to the sample magnetization and B_{obs} is given by a summation of $\mu_0 M$, $\mu_a H$, and $\mu_0 H$ due to the ferromagnetic α'-martensites, austenitic matrix, and applied field, respectively as shown in Fig. 3(a). Here, μ_0 and μ_a denote the permeability of vacuum and the austenitic matrix, respectively. Consequently, the properties of B_{obs}-H loop i.e. the remanence work $W_{R,B}^*$, magnetization B_a^* and coercive force $H_{c,B}^*$ shown in Fig. 3(a), are largely different from the corresponding W_R*, $\mu_0 M_a^*$ and H_c^* in the $\mu_0 M$-H loop, whereas other properties W_F^* and M_R^* are not influenced by the austenitic matrix and applied field. The scaling rules of (1) will therefore no longer hold true. Figures 4(a) – 4(c) show double logarithmic plots of relations between W_F^*

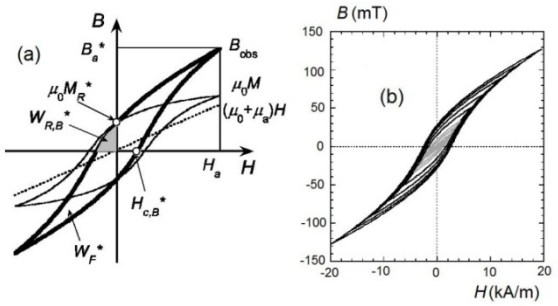

Fig. 3. (a) Schematic diagram of the hysteresis loops and the parameters of the B_{obs}-H loop. In addition to $\mu_0 M$ (thin line) due to ferromagnetic α'-martensites, both $\mu_a H$ and $\mu_0 H$ (dotted line) are involved in the B_{obs}-H (thick line) loop. The parameters $W_{R,B}^*$, B_a^* and $H_{c,B}^*$ in the B_{obs}-H loop are also shown to distinguish from W_R^*, M_a^* and H_c^* in M-H curve, respectively. (b) A set of minor hysteresis loops. The data for 502 MPa are given as an example. Minor loops with H_a below 4 kA/m (gray loops) were used to obtain W_m^0.

and B_a^*, $W_{R,B}^*$ and M_R^* , and $H_{c,B}^*$ and M_R^*, respectively, taken for various levels of stress. Unlike ferromagnetic materials, no linear part was detec-ted over the entire range of B_a^* in the W_F^* and B_a^* curves. The double logarithmic plots of the $W_{R,B}^*$-M_R^* and $H_{c,B}^*$-M_R^* curves show the linear behavior in a limited range of M_R^*. However, the exponents n_R and n_c, determined from least-squares fits using (1) show a high value of 1.9 and 0.9, respectively, and monotonically decrease with increasing volume fraction of α'-martensite; as the volume fraction increases from 1.5 to 19.5%, n_R and n_c decreases from 2.0 to 1.8 and from 0.97 to 0.76, respectively. The observation shows that the scaling rules given by (1) are not universal for deformed 304 stainless steels where ferromagnetic α'-martensites are induced. This is attributed to the fact that the paramagnetic austenite matrix and applied field are also involved in the value of B_a^*, W_R^*, and H_c^*. Actually, with increasing the volume fraction, both n_R and n_c approach the values of 1.5 and 0.45 for ferromagnetic materials, respectively. On the other hand, the two minor-loop parameters M_R^* and W_F^* only reflect the property of α'-martensites. Therefore, a magnetic property obtained from the relation may reveal the intrinsic features of α'-martensites. Figure 4(d) shows the relation plotted on a double logarithmic scale for various levels of stress. One clearly see that the W_F^*-M_R^* curves exhibit straight lines over a wide range of W_F^* and M_R^* and the slope is almost independent of volume fraction. This range shifts toward higher values with increasing applied stress because both parameters are proportional to the volume fraction of α'-martensites. This linearity strongly indicates the presence of a scaling power-law rule between W_F^* and M_R^*. In order to extract the intrinsic magnetic properties of α'-martensites, we assume the equation given by (7). Least-squares fits to (7) yielded an almost constant value of n_m = 1.40 ± 0.04. Here, minor loops with H_a below 4 kA/m shown in Fig. 3(b) were used for the fits. This value is independent of the volume fraction of α'-

martensites, strongly indicating the presence of a universal scaling power law rule for strain-induced α'-martensites.

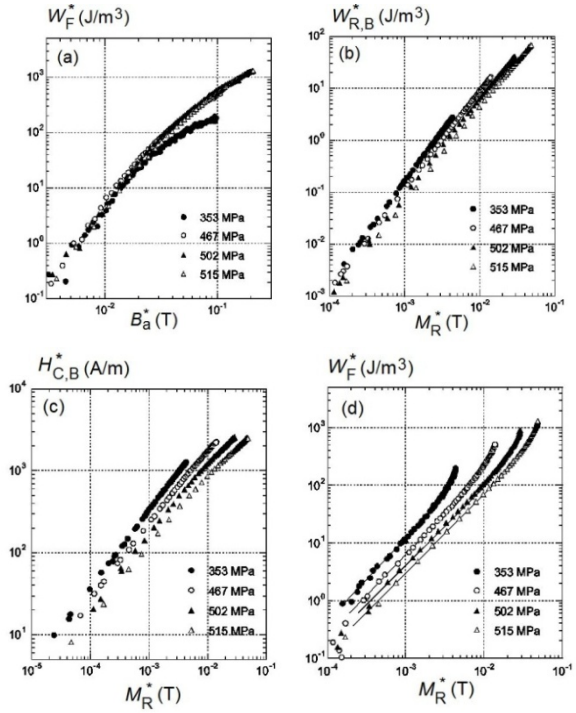

Fig. 4. The relations (a) between W_F^* and B_a^*, (b) between $W_{R,B}^*$ and M_R^*, (c) between $H_{c,B}^*$ and M_R^*, and (d) between W_F^* and M_R^*, plotted on a double logarithmic scale. The solid lines in (d) denote the least-squares fitting lines.

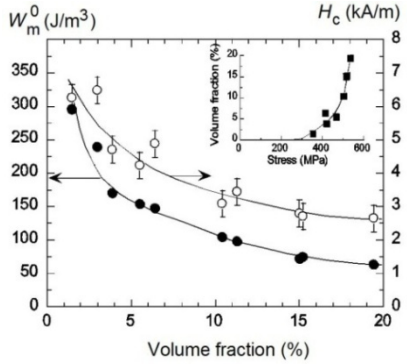

Fig. 5. W_m^0 as a function of the volume fraction of α'-martensites. For comparison, H_c obtained from the saturation magnetization measurements is also given. The inset shows the volume fraction as a function of stress.

To investigate the physical meaning of the minor-loop coefficient of (7), W_m^0 as a function of the volume fraction is plotted in Fig. 5. W_m^0 sharply decreases with volume fraction below 3% and then slowly decreases up to a maximum volume fraction of 19.5%. This trend is similar to that of H_c obtained from the saturation magnetization measurements with SQUID magnetometer. However, the decrease in W_m^0 from 1.5 to 19.5% fraction is approximately 80% and much larger than 58% in the case of H_c. This indicates the high sensitivity of W_m^0 to ferromagnetic α'-martensites. It should be noted that the measurement field to obtain W_m^0 is below 4 kA/m and far lower than ~ 1 MA/m required to obtain H_c in general. During plastic deformation, an austenitic structure (γ) transforms into α'-martensites by shearing the lattice. At the initial stage of plastic deformation, small α'-martensite particles are nucleated around the intersection of the shear bands [8]. As the plastic deformation progresses, α'-martensite particles grow, merge with each other, and form larger clusters. When the volume fraction is low, α'-martensite particles (clusters) can be considered to be isolated ones with no inter-particle interactions. In this case, H_c would be mainly determined by the size [9,10] because the pinning strength of the magnetic domain walls at the α'-γ boundaries weakens with the volume-to-surface ratio. The decrease in H_c with increasing volume fraction therefore reflects an increase in the particle (cluster) size. Since W_m^0 has a good proportional relation with H_c, W_m^0 is good indicators of the morphology of α'-martensites.

4 CONCLUSION

A new scaling power-rule between hysteresis loss and remanence of minor hysteresis loops was proposed to investigate minor-loop properties of ferromagnets where previous scaling rules do not hold true. The analysis for Co and strain-induced α'-martensites revealed that the power-law exponent is about 1.4 and universal, being independent of types of ferromagnets. The coefficient of the power-law shows a similar behavior to the structure-sensitive property, coercive force, and can be obtained with magnetic fields far lower than the saturation field. The magnetic method using this scaling rule can be an useful technique for nondestructive evaluation of ferromagnetic structural components because of the sensitivity and low measurement fields.

Acknowledgement

The Co single crystal was prepared under the inter-university cooperative research program of the Advanced Research Center of Metallic Glasses, Institute for Materials Research, Tohoku University.

REFERENCES

[1] STEINMETZ, C.P., Proc. IEEE **72** (1984), 197-221.
[2] TAKAHASHI, S. – KOBAYASHI, S. – KAMADA, Y. – KIKUCHI, H. – ZHANG, L. – ARA, K., Physica B **372** (2006), 190-193.
[3] KOBAYASHI, S. – FUJIWARA, T. – TSUNODA, M. – TAKAHASHI, S. – KIKUCHI, H. – KAMADA, Y. – ARA, K. – SHISHIDO, T., J. Mag. Mag. Mater. **310** (2007), 2638-2640.
[4] KOBAYASHI, S. – KIMURA, T. – TAKAHASHI, S. – KAMADA, Y.– KIKUCHI, H., J. Mag. Mag. Mater. **320** (2008), e551-e555.
[5] BALL, J.D., Gen. Elec. Rev. **19** (1916), 369-390.
[6] FOSTER, K., J. Appl. Phys. **55** (1984), 2127-2129.
[7] BOZORTH, R.M., *Ferromagnetism* (IEEE, New York 1978)
[8] MANGONON, P.L., – THOMAS, G., Metall. Trans. **1** (1970), 1577-1586.
[9] TAVARES, S.S.M. – DA SILVA, M.R. – NETO, J.M. – MIRAGLIA, S. – FRUCHART, D., J. Mag. Mag. Mater. **242-245** (2002), 1391-1394.
[10] ZHANG, L. – TAKAHASHI, S. – KAMADA, Y., Scripta Mater. **57** (2007), 711-714.

Received 28 June 2008